A thermo-chemical exploration of a two-dimensional reacting supersonic mixing layer

Debasis Chakraborty,[a] H. V. Nagaraj Upadhyaya, P. J. Paul, and H. S. Mukunda
Department of Aerospace Engineering, Indian Institute of Science, Bangalore—560 012, India

(Received 2 December 1996; accepted 7 July 1997)

The hypervelocity two-dimensional reacting supersonic mixing layer experiments of Erdos *et al.* with a H_2/air stream have been simulated with model free fine grid calculations on a N–S solver with full and single step chemistry. Response of the flow to fluctuations in the in-flow stream is utilized to examine chemistry fluid flow interactions. A favourable comparison of the computation with experimentally measured wall static pressure and heat transfer data along with flow picture forms the basis for further analysis. Insight into the mean flow thermal and reaction properties is provided from the examination of large scale structures in the flow in which the hydrogen stream is at 103 K flowing at 2.4 km/s ($M=3.09$) and the air stream is at 2400 K flowing at 3.8 km/s ($M=3.99$). The chemistry-flow interaction is dominated by large stream kinetic energy and affects the mean properties including the temperature profiles across the mixing layer. Single step chemistry, in comparison to full chemistry, is inadequate to describe ignition and early combustion processes, but seems reasonable for describing mixing and combustion downstream. Fast chemistry approximation coupled with mixture fraction based on hydrogen element seems to predict H_2 mean profiles well; but this is shown to be due to the insensitivity of Y_{H_2} to progress of the reaction. This approximation under-predicts Y_{O_2} though the general shape of the profile is maintained. Mixture fraction variable approach is shown to be inadequate for the prediction of the H_2O mass fraction because of the effect of non-normal diffusion. Finite chemistry conditions are shown to prevail throughout the domain of the mixing layer. It appears that use of mixture fraction approach may be inadequate to compute high speed reacting turbulent flows. © *1997 American Institute of Physics.*
[S1070-6631(97)01111-2]

I. INTRODUCTION

Supersonic reacting flows have been explored experimentally[1–3] and computationally[4–7] and in the recent times on the modeling aspects.[8–10] Two experimental studies which have been explored computationally are the experiments of Burrows and Kurkov[1] and of Evans *et al.*[11] In the former case, H_2 comes off as a wall-jet with the free stream consisting of high temperature vitiated air. The turbulent diffusion flame is examined by measurements of velocity, temperature, and species mass fractions at two stations downstream of the injection point. In this case, it may be expected that the wall boundary layer has a significant influence on the structure of the flame. Evans *et al.*[11] conducted experiments on a co-flowing jets of H_2 and air streams at high temperature and measurements of composition of major species and temperature have been performed. In this case there are not many measurements for comparison. In a subsequent work Cheng *et al.*[2] have presented a whole set of very useful data on a similar geometry. These consist of simultaneous measurements of mean and fluctuations of temperature and species—major as well as minor—using non-intrusive diagnostics but do not include velocity measurements. These results on co-flowing jets have not been examined computationally. The above experiments are limited to stream Mach numbers of 2 or less. Another important experiment on hypervelocity mixing layer is the work of Erdos *et al.*[3] in which gaseous H_2 and air at Mach numbers of 3.09 and 3.99 flow off a splitter plate in a 25.4 mm high rectangular test section of more than 500 mm length. Measurements are limited to wall static pressures and heat flux. Flow visualisation using laser holographic interferometry and pictures of schlieren and shadowgraph as well as finite and infinite fringe interferometry have been presented. While it is true that detailed profiles of thermochemical variables are unavailable, the cleanliness of the geometry and the flow visualisation, along with wall pressure history, provide enough incentive to examine through computational techniques the hypervelocity experiment.

Exploration of the thermo-fluid behavior on supersonic mixing layers has been made by Sekar and Mukunda[6] and Vuillermoz *et al.*,[7] modeling aspects have been treated by Zheng and Bray,[8–10] and a summary of these aspects is available in Bray.[10]

II. CONSIDERATIONS FOR SIMULATION

Though Erdos *et al.*[3] have studied mixing layers with a H_2 stream on one side and N_2, O_2, and air streams on the other side, in this work we deal with the simulation of the H_2/air system only. The details of inflow parameters is shown in Table I. The convective velocity is 3000 km/s and the convective Mach numbers are 0.85 and 0.82 referred to as H_2 and air streams, respectively. The free shear layer experiments of Clemens and Mungal[12] suggest dominant three-dimensional effects for this convective Mach number range and have been supported by the linear instability

[a]External student from ARD, VSSC, Thiruvananthapuram.

Downloaded 13 Feb 2007 to 203.200.43.195. Redistribution subject to AIP license or copyright, see http://pof.aip.org/pof/copyright.jsp

TABLE I. Inflow parameters.

Species	u, km/s	T, K	M	p, MPa	Re/mm
H_2	2.4	103	3.09	0.021	1600
Air	3.8	2344	3.99	0.021	22000

analyses[13,14] which have shown that oblique disturbances become more and more unstable as the convective Mach number exceeds 0.6. However, Tam and Hu[15] and Zhuang *et al.*[16] have shown that, for laterally confined mixing layers, the most unstable mode is the lowest order two-dimensional mode. The principal point made in these papers is that the coupling between the motion of the shear layer and the channel acoustic wave produces a new instability mechanism in the supersonic range which originates from the wall confinement and is different from the classical Kelvin–Helmholtz instability. Zhuang *et al.*[16] have shown that the bounded two-dimensional modes are in good agreement with the experiments of Papamoschou and Roshko.[17] Lu and Wu[18] have performed two-dimensional simulations for a mixing layer with a convective Mach number as high as 1.77 citing the work of Tam and Hu[15] who studied the effect of confinement on the shear layer development in supersonic streams. Recently, Liou *et al.*[19] have conducted a two-dimensional computational study of the compressibility of high speed mixing layers. These studies have shown that two-dimensional simulation is satisfactory for confined mixing layers.

In the present work, both confinement and heat release effects are part of the physics implying that the role of large scale two-dimensional structures in modulating the chemistry–flow interactions is significant and can be understood from two-dimensional simulations.

The simulations are made for a H_2/air system first without chemical heat release, then with single step chemistry (SSC) and this followed by detailed chemistry (FC). A point which has been debated in the literature is the need for full chemistry in capturing the heat release effects in high speed flows. Because the time scales of flow and diffusion available become shortened with an increase in speed, chemistry tends to be controlling. But the fact that in these situations, one uses high temperatures—1500 K or more—it is likely that chemistry becomes fast and one can use simpler models. Recently Ju and Nioka[20] have shown that a reduced chemistry model might be adequate in describing ignition dynamics in the mixing layer. The reduced chemistry model might be adequate for describing combustion dynamics downstream as well since the fine details of chemistry are much more important for ignition. Mukunda[21] based on short length simulations of reacting flow with FC concluded that fast chemistry may be a poor approximation due to strong stretch effects in the large scale structures. Zheng and Bray[9] concluded that fast chemistry is inadequate for making quantitative predictions and a flamelet model can improve the predictions for high speed reacting flows. The conclusions would have been more authentic had they treated the experiments of Cheng *et al.*[2] where the data is far more extensive.

The present work therefore aims at obtaining the simulation results for the following.

(1) A geometry which has adequate length for the flow to develop.
(2) Make experimental comparisons to ensure the validity of the study.
(3) Examine the chemical aspects along with flow structure in some detail.

III. THE CODE AND COMPUTATIONAL DETAILS

The code used in the present calculations is the SPARK2D combustion code developed at the NASA LaRC by Drummond and Carpenter[4] and has already been used in Sekar and Mukunda[6] and Mukunda.[21] It uses a 4th order compact MacCormack scheme with second order temporal accuracy. This choice represents a compromise between the accuracy of higher order numerical algorithms and the robustness and efficiency of lower order methods. The code has been validated by computing a linearly unstable shear flow problem in the early stages of the growth. Carpenter and Kamath[22,23] have demonstrated that, with the compact schemes considered here, the growth rates with the initial profiles based on the eigenfunctions predict those from linear stability theory for free shear layers to within 1% for a time duration equal to about five times the sweep time of the flow field. This accuracy is adequate for the present computations needing a maximum of three sweep times—one sweep for clearing the flow field, and two more sweeps to collect statistical information and also check on the statistical invariance of the calculations.

The boundary conditions set for the present problem are different from those in Sekar and Mukunda[6] in that in this case, the region is confined; zero slip conditions and constancy of wall temperature are imposed on the wall. The lower stream is of air (from 0 to 12.7 mm height) and the upper stream is of H_2 (from 12.7 to 25.4 mm height). On the inflow stream is imposed velocity fluctuations over a range of frequencies at a total rms intensity of 0.3% of the mean velocity as shown in Fig. 1, in which is shown the velocity vs the time plot Fig. 1a) and the normalized frequency vs the amplitude plot (Fig. 1b). The frequency has been normalized with the mean velocity to the channel width ratio. It can be seen that the input fluctuations have many components up to the normalized frequency of 0.003. The frequency range allows the mixing layer to grow as may happen in reality. The exit boundary condition is obtained by second order extrapolation and is considered satisfactory for this problem dominated by supersonic flow.

The reaction rates have been have been calculated using both single step chemistry and full chemistry models. A reaction mechanism involving six species and seven reversible reactions[4–6] has been chosen for the full chemistry calculations. The reaction steps and the rate parameters of the reactions are given in Table II. For single step chemistry calculations the following reversible reaction has been chosen:

$$2\,H_2 + O_2 \rightleftharpoons 2\,H_2O,$$

and the net rate of reaction of H_2 (in kg-mol/m^3 s) is given by the expression[4–6]

Downloaded 13 Feb 2007 to 203.200.43.195. Redistribution subject to AIP license or copyright, see http://pof.aip.org/pof/copyright.jsp

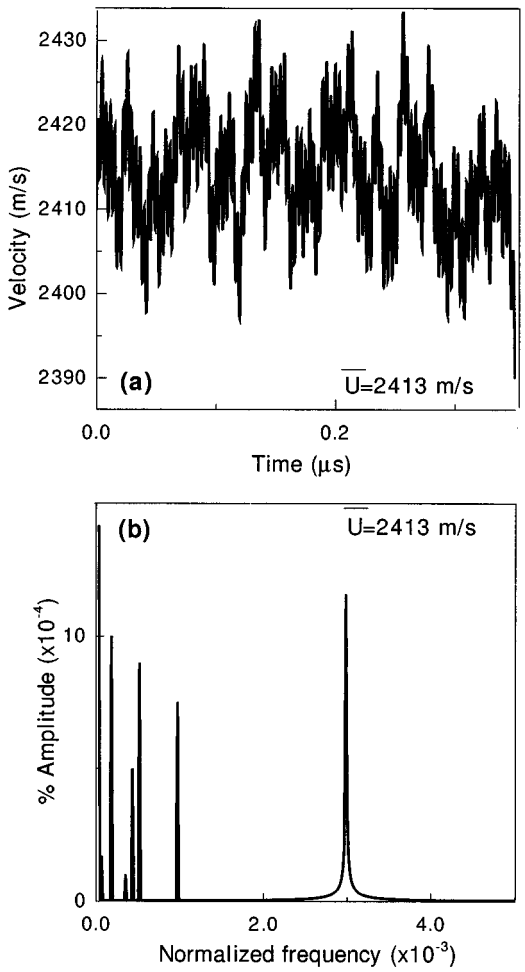

FIG. 1. The imposed velocity fluctuations at the in-flow plain (a) velocity vs time (b) fourier transform of velocity fluctuations.

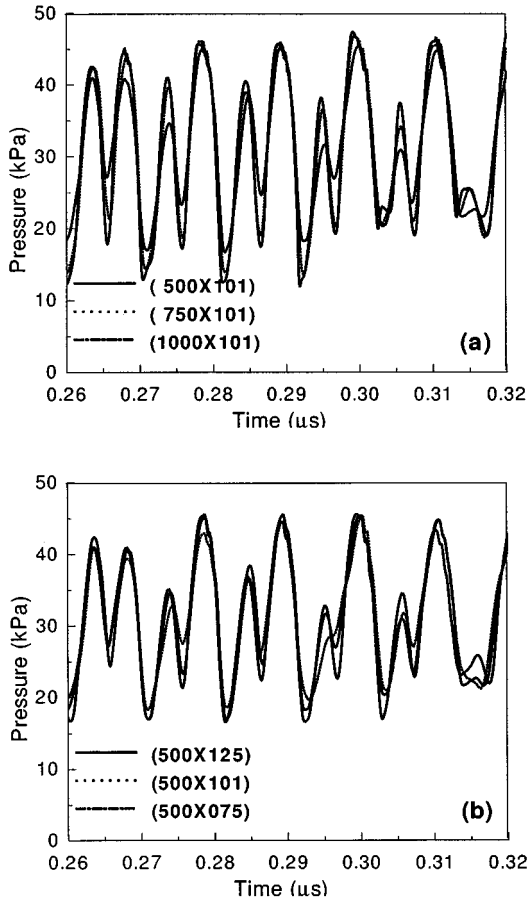

FIG. 2. The pressure vs time obtained with grid refinements. (a) With grid refinements in the axial direction. (b) With grid refinements in the cross-stream direction.

$$\frac{dc_{H_2}}{dt} = -2[1.102\times 10^{19}\exp(-8052/T)c_{H_2}^2 c_{O_2} - k_b c_{H_2O}^2], \quad (1)$$

where c is the molar concentration (in g-mol/cm^3) and k_b, the rate constant of the reverse reaction, is obtained from the forward rate constant and equilibrium constant.

The grid structure has 1000 grid points of 0.3 to 0.8 mm size along the length of 535 mm with the smaller sizes arranged to allow the boundary layer coming-off the splitter plate to develop without numerical problems. There are 101 grid points in the cross-stream direction with 0.09 to 0.5 mm size, the smaller sizes being in the middle zone of height. These are finer or about the same as in the earlier computations which allowed a good capture of the large scale structures as well as the reaction zones. Grid resolution calculations were made by varying the number of grids both in the axial and cross-stream directions. Figures 2a and 2b show the effect of grid refinements in axial and cross-stream directions, respectively, on temporal variation of pressure. As can be seen, increasing the number of grids from 750 to 1000 in the axial direction and from 101 to 125 in the cross-stream direction leave the results almost unchanged.

A further comparison on the effect of grid size on the spectral content of the pressure fluctuations are shown in Figs. 3a and 3b for axial and cross-stream grid refinements. The amplitudes are normalized by the mean and the frequency by the ratio of a characteristic thickness to mean velocity. The characteristic thickness is taken as the channel width. Even the spectral content of the fluctuations is well tracked except at high frequencies. Hence, the calculations are model free except at very small scales which are unlikely to affect the large scale structure of the flow. The grids chosen namely 1000×101 give a good representation of the

TABLE II. Elementary reactions and reaction rate parameters used for full chemistry computations. The rate constant k is obtained as $k=AT^b\exp(-E/RT)$ where k has the units (g-mol/cm^3)$^{-(n-1)}$/s. The reverse rate constants are determined from the forward rate constants and the equilibrium constants of the reaction.

No.	Reaction	A	b	E/R
1.	$H_2+O_2\rightarrow OH+OH$	0.170×10^{14}	0.	24230
2.	$O_2+H\rightarrow OH+O$	0.142×10^{15}	0.	8250
3.	$H_2+OH\rightarrow H_2O+H$	0.316×10^{8}	1.8	1525
4.	$H_2+O\rightarrow OH+H$	0.207×10^{15}	0	6920
5.	$OH+OH\rightarrow H_2O+O$	0.550×10^{14}	0	3520
6.	$OH+H+M\rightarrow H_2+M$	0.221×10^{23}	-2	0
7.	$H+H+M\rightarrow H_2+M$	0.655×10^{18}	-1	0

Downloaded 13 Feb 2007 to 203.200.43.195. Redistribution subject to AIP license or copyright, see http://pof.aip.org/pof/copyright.jsp

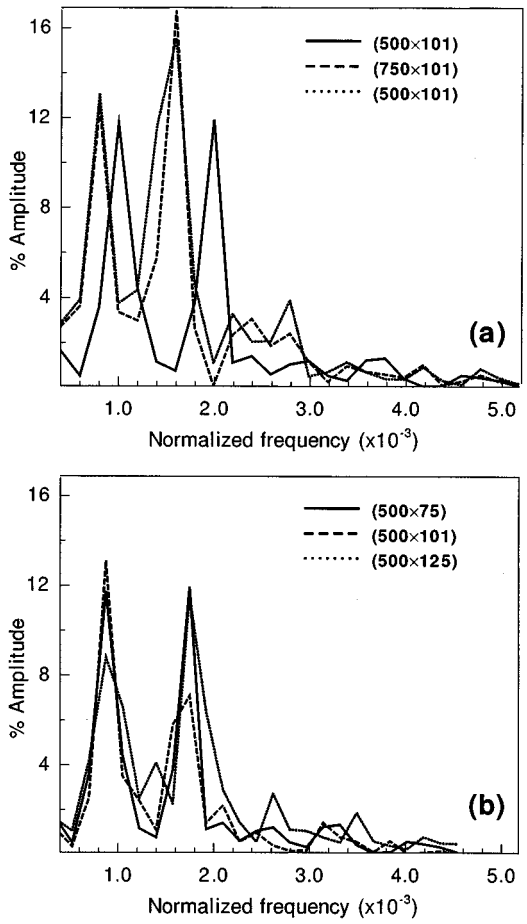

FIG. 3. The spectral distribution of fluctuations on an amplitude vs normalized frequency plot (a) with grid refinements in the axial direction. (b) With grid refinements in the cross-stream direction.

temporal evolution of the flow field. An additional feature of Figs. 3a and 3b is that the amplitude of fluctuations downstream goes up to 12%–15%, where as the total rms inflow velocity fluctuations are only 0.3% of the mean, and the frequency content of the downstream fluctuations is much richer than in the inflow. Similar comparisons of velocity fluctuations downstream have shown similar good results for 1000×101 grids. Hence it is concluded that the 1000×101 grid chosen here is sufficient to give grid-independent solutions.

As in the earlier studies,[6,21] the code is run through over one sweep to obtain a statistical steady state and data on velocities, temperature, and mass fractions are gathered at several points and sections of the flow for next one/two sweeps at each time step to enable statistical analysis. In the analysis of the results, the element and mixture fraction variables are made use of. The mass fraction of element i is given by[8]

$$z_i=\sum_{i=1}^{n}\frac{\alpha_{ij}A_i}{M_j}Y_j, \tag{2}$$

where α_{ij} is the number of atoms of element i in a molecule of specie j, A_i is the atomic mass of the element i, and M_j is the molecular mass of specie j. The normalized element fractions are defined as

$$Z_i=\frac{z_i-z_{iu}}{z_{il}-z_{iu}}, \tag{3}$$

where z_{iu} and z_{il} refer to the mass fraction of the element i in the incoming upper and lower streams, respectively. With the knowledge of mass fractions of the species, it is possible to compute z_i and therefore, Z_i.

For computing the probability density function, the values of mass fractions and temperature at selected locations are stored at every step after obtaining statistically steady flow. Mean and standard deviation are computed from these time series data. The probability density function is calculated from the histogram of the variable over its valid range. The value of the probability density function at the midpoint of a class interval is taken as the class frequency divided by the total number of samples divided by the class interval. In order to assess the validity of the thin flame approximation (fast chemistry), the mass fractions are computed using this approximation and averaged over the mixture fraction space. The mass fractions as function of Z for fast chemistry are obtained for the hydrogen–air system as

$$Y_f(Z)=1-Z/(Z_s), \tag{4}$$

$$Y_{ox}(Z)=0.231(Z-Z_s)/(1-Z_s). \tag{5}$$

In the above equations Z stands for Z_{H}. The quantities Y_f and Y_{ox} are the fuel and oxidiser mass fractions, respectively. The average values are obtained by integrating the mass fractions weighted with the probability density function $P(Z)$ over Z,

$$\overline{Y_i}=\int_0^1 Y_i(Z)P(Z)dZ, \tag{6}$$

where Z_s, the mixture fraction at stoichiometry, is given as $Z_s=s/(s+0.231)$, with s, the stoichiometric ratio ($=8$ in the present case). Attempts are made to examine if the generally recognised β function to represent the probability density function would be a good representation. It is defined by

$$P(z)=\frac{z^{\alpha-1}(1-z)^{\beta-1}}{\int_0^1 z^{\alpha-1}(1-z)^{\beta-1}dz}. \tag{7}$$

The parameters α and β can be related to the mean and the mean square fluctuations of Z as

$$\alpha=\overline{Z}\left[\frac{\overline{Z}(1-\overline{Z})}{\overline{Z'^2}}-1\right], \tag{8}$$

$$\beta=\alpha\left(\frac{1}{\overline{Z}}-1\right), \tag{9}$$

where $\overline{Z}$ is the average of the mixture fraction Z and $\overline{Z'^2}=\overline{Z^2}-\overline{Z}^2$ is the mean square fluctuation of Z.

Downloaded 13 Feb 2007 to 203.200.43.195. Redistribution subject to AIP license or copyright, see http://pof.aip.org/pof/copyright.jsp

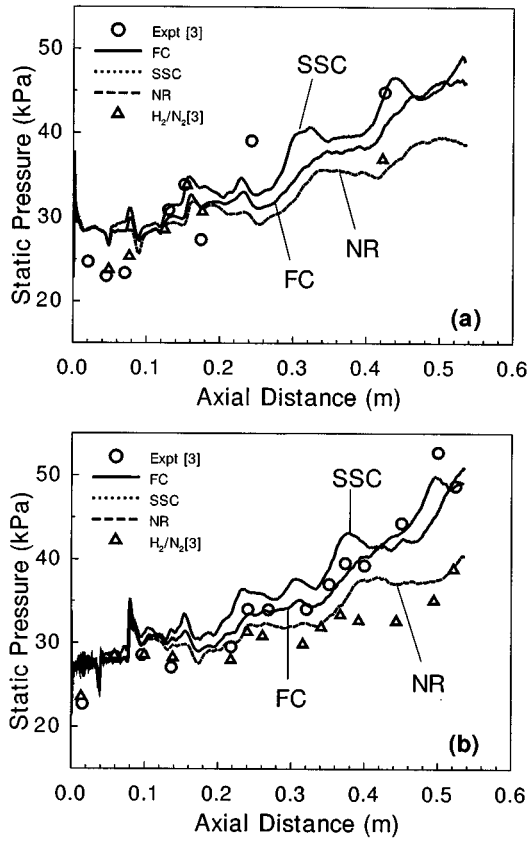

FIG. 4. Variation of wall static pressure with axial distance—experimental results of Erdos *et al.* Predictions for full chemistry and single step chemistry. (a) At the upper wall; (b) at the lower wall.

IV. RESULTS AND DISCUSSION

The wall pressure variation obtained from the calculations are presented for SSC (Single Step Chemistry) and FC (Full Chemistry) NR (nonreacting) cases with the experimental data in Fig. 4. The no-reaction experimental results corresponds to the H_2/N_2 system. The flow has adverse pressure gradient due to heat release and wall friction. Predicted wall pressure on the upper wall (H_2 side) match better with the experimental data compared to the lower wall. Considering the repeatability of experimental data as evidenced in other experimental data,[3] the comparison can be taken as being reasonably good. The SSC case has a higher pressure rise in comparison to the FC case. Most experiments on scramjets use this behavior to determine if heat release has occurred in the system.[24] The computational results show the presence of a leading shock wave attached to the splitter plate at an angle of 20° to the horizontal which is consistent with the experiment.

Figure 5 is a composite picture containing the contour plots of water mass fraction, temperature, heat release rate, and two derived parameters D and E defined as

$$D = \nabla Y_{H_2} \cdot \nabla Y_{O_2}, \tag{10}$$

$$E = Y_{H_2} Y_{O_2} / z_H z_O, \tag{11}$$

for full chemistry [Fig. 5(a)] and single step chemistry [Fig. 5(b)]. The first term, D, is the dot-product of the gradients of fuel and oxidiser mass fractions. In a recent study, Yamashita *et al.*[25] used this index to determine the zones of premixedness and diffusion dominated combustion in a mixing layer. The basic idea is that if the quantity is strongly negative, then the zone is dominated by diffusive combustion since the flame zone is being fed by the oxidant and fuel from opposite directions; if the quantity is strongly positive, the zone is affected by premixed combustion since the fuel and oxidiser are being fed from the same side. The second term, E, gives a measure of the unreacted mass in the mixed fluid. The denominator $z_H z_O$ is indicative of the extent of mixing of the two streams, while $Y_{H_2} Y_{O_2}$ indicates the unreacted part of the mixed fluid. Outside the mixing layer, the denominator will be zero and in these regions E is also set to zero. In the case of no-reaction, E will be unity in the mixed zone and in the case of fast chemistry, E will be zero throughout the field, since then H_2 and O_2 will not co-exist.

Figure 5 shows the plots both for single step and full chemistry calculations so that direct comparison of many features is possible. The distribution of water mass fraction shows far more extensive development with full chemistry than the single step, particularly towards the end of the channel. There is a near complete engulfing of the fluid in the channel in the case of full chemistry in comparison to single step chemistry. While the temperature contours for FC and SSC appear similar, there are differences which influence the heat release distribution discussed below. A large number of the vortical structures have temperatures between 500 and 1500 K. The upper regions are at 103 K and the lower zones at 2400 K and above the rise near the wall being caused by boundary layer heating.

The heat release plots are interesting. A negative sign refers to the exothermic heat release. Positive regions refer to endothermic chemical processes. In the case of a single step reaction, the mechanism for endothermic process—reverse reaction—is very weak, because of the absence of intermediate species. One can see a high heat release zone as a white marked sheet (not too thin). In the case of FC, one can discern both exothermic and endothermic zones clearly shown up on the hydrogen and air sides, respectively. The very high temperature zones on the air side are mostly endothermic, understandably since dissociation dominates these zones with a very small amount of fuel. The equilibrium constants of the reactions have a high heat of the reaction change by more than two orders by increasing the temperature from 2500 K to 3000 K. Hence the reactions which are exothermic at lower temperatures become endothermic at higher temperatures wherein backward reactions would be dominating.

Plots of $Y_{H_2} Y_{O_2} / z_H z_O$ show in the case of single step chemistry, a number of vortical structures with a low value of this parameter indicating closeness to the complete reaction. In the case of full chemistry, however, many vortical structures have a not-too-small value of this parameter (0.3 to 0.5) and spotty zones with high values indicating near no-reaction and full mixedness. A combined examination of the above plot with that of the heat release rate shows the vortical structures are composed of a mixed fluid only partly reacted and the high heat release zone is along the edges of the vortical structures than the central zone.

Downloaded 13 Feb 2007 to 203.200.43.195. Redistribution subject to AIP license or copyright, see http://pof.aip.org/pof/copyright.jsp

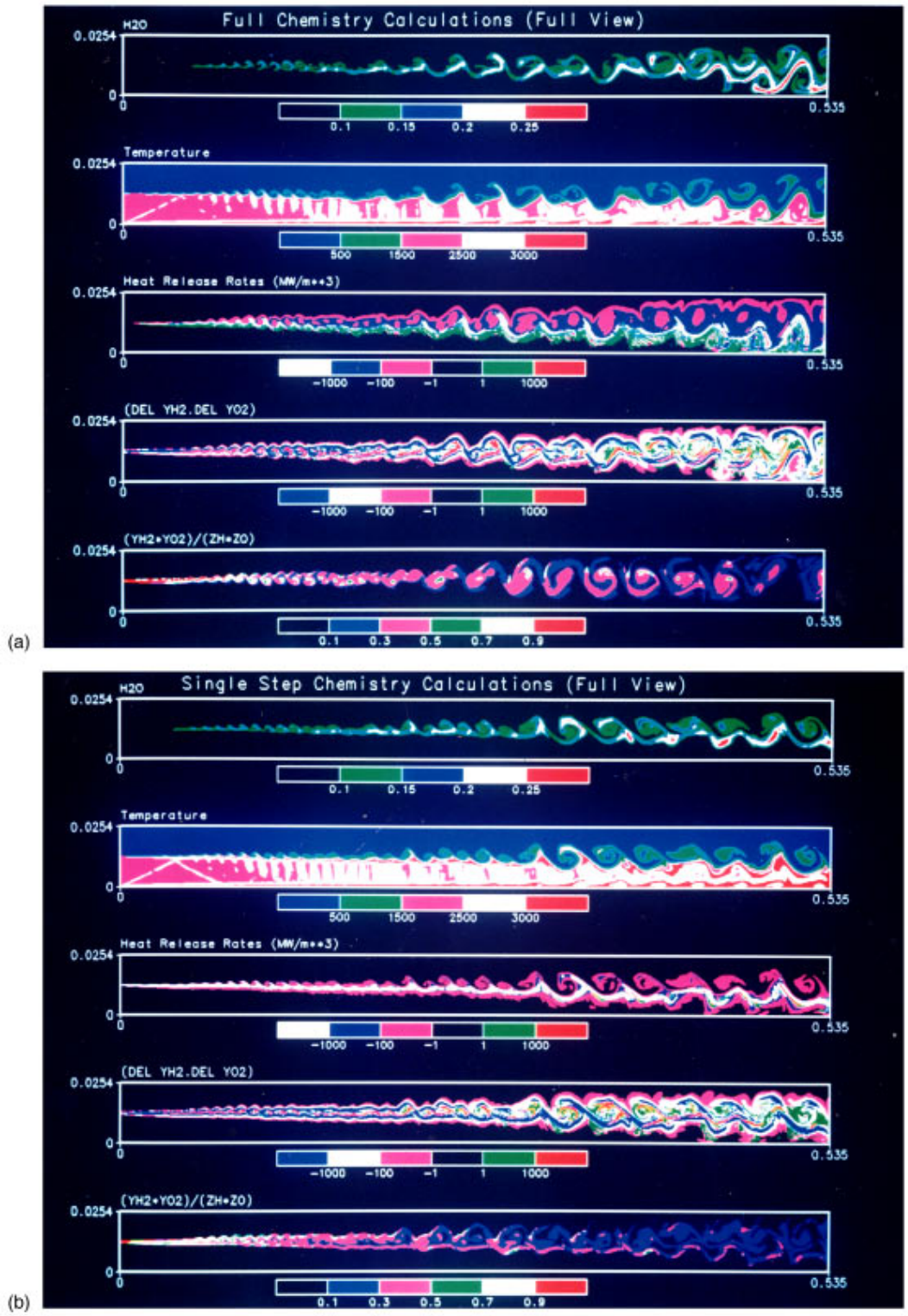

FIG. 5. Contour plots of the H_2O mass fraction, temperature, heat release rates, D, and E in the test section for FC (a) and SSC (b).

The features described so far are also seen in the plot of $\nabla Y_{H_2} \cdot \nabla Y_{O_2}$. The plot shows a range of levels, both diffusive and premixed zones. The premixed zones are weak and the diffusive layers are more intense. The blue coloured sheets are similar in likeness to high heat release zones indicating that it is the diffusive layers which are contributing to high heat release.

Dimotakis and Hall[26] have suggested that in high speed mixing layers, due to very high strain rates, reactions take place not in the outer layers of the vortices, where the fuel and the oxidiser first come in contact, but in the central zone in a near pre-mixed mode. The results of the simulation shown in Figs. 5a and 5b do not support this view point. The premixed zones are small and the reaction sheets are largely

Downloaded 13 Feb 2007 to 203.200.43.195. Redistribution subject to AIP license or copyright, see http://pof.aip.org/pof/copyright.jsp

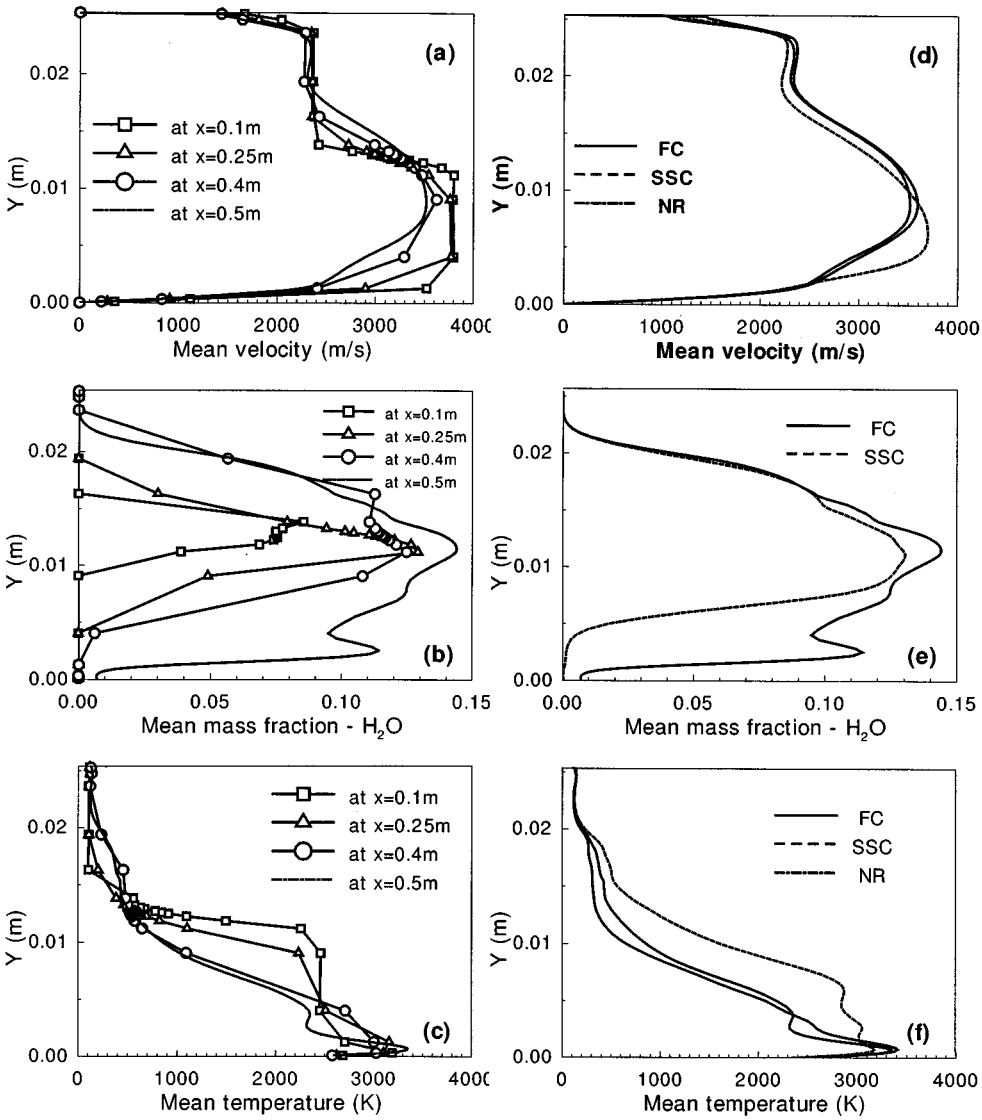

FIG. 6. Variation of the mean profiles through the mixing layer and comparisons of these profiles with different cases. (a), (b), (c) Cross-stream distribution of mean velocity, H_2O mass fraction, and temperature at different axial distances for FC. (d), (e), (f) Comparison of FC, SSC, and non-reacting cases at $x=0.5$ m.

diffusive in character. The reason for this deviation from the Dimotakis and Hall model, possibly, is that air stream is at a very high temperature (the static temperature of 2344 K) and hydrogen at a very low temperature (103 K), so that the reacted stream temperature is not greater than the air stream as seen from the temperature contours in Figs. 5a and 5b.

The mean quantities are computed by averaging the data over one sweep and are presented in Fig. 6 for both SSC and FC at various locations. As the layer is growing with distance, smoothing of the velocity profile, an increase in the velocity of the H_2 stream and a decrease in the air stream are clear. The layer has grown more into the air side as is clear from the unchanged profile region on the hydrogen side. This implies more of high speed fluid being found in the mixing layer a feature described by Koochesfahani *et al.*[27] The water mass fraction profiles have grown to nearly the full width of the channel leaving a small section on the hydrogen side unpenetrated in the mean. The mean water fraction profile growth rate (δ_{H_2O}/x) is about 0.055–0.045 with the larger values for shorter distances and the smaller values are those taken over larger distances. Estimates of the growth rate from results of Brown and Roshko[28] with the necessary compressibility corrections show values of 0.03 to 0.035 (Ref. 29) allowing for uncertainties in the growth rate of incompressible mixing layer. It appears as though the growth rate is larger than typical estimates. Perhaps the effects of an adverse pressure gradient have resulted in enhanced growth rate of the mixing layer.

The temperature profile is perhaps the most dramatic with an upper stream at 103 K and the lower stream at 2400 K, the process of boundary layer growth on the lower wall raised the temperature to values in excess of 3200 K. However, the temperature in most other zones decreases from the profiles at start largely because of large scale structures causing significant mixing with the cold stream. Yet the water

Downloaded 13 Feb 2007 to 203.200.43.195. Redistribution subject to AIP license or copyright, see http://pof.aip.org/pof/copyright.jsp

mass fraction profiles show significant amounts of H_2O produced in the mixing layer. These are the results of non-normal diffusion—hydrogen and water vapour with a lower molecular mass (much lower in the case of hydrogen) compared to the local average value diffuse at higher rates and therefore cause effects leading to profiles of the water mass fraction not uniquely related to temperature (it will be linearly related to temperature if the effective diffusion was normal, i.e., Lewis number=1).

The lower figures (Figs. 6d,e,f) show a comparison of the profiles at $x=0.5$ m for FC, SSC, and no-reaction cases. It appears that changes because of FC are marginal and SSC, slightly significant in comparison with the no-reaction case. The reason lies in the fact that, in high enthalpy flows of the kind considered here, enthalpy changes due to chemistry are not large compared to the total enthalpy. To illustrate this point, it is useful to appreciate that the sensible enthalpy of the air and H_2 streams are about 1.93 and 1.65 MJ/kg where as the kinetic energies are 7.2 and 2.9 MJ/kg. A change of 10%–15% of the free stream speed (the change at the peak velocity region) corresponds to a change in enthalpy of 1.4 to 2 MJ/kg which is about the same as the magnitude of the sensible enthalpy itself. This aspect has been addressed first in Ref. 6 and also by Zheng and Bray[9] when they indicate the need to consider changes in kinetic energies in the calculations of chemistry–turbulence interactions. The growth of the water mass fraction profile is more significant for FC than for SSC. This is due to mixing being inhibited by heat release in the early parts of the mixing by the relatively faster FC. This feature is also noticed with H_2O contour plots for SSC. The comparison of the temperature profiles is again very interesting. The temperature profile with FC is close to that with no reaction. For the SSC case the temperatures locally are much higher. The reasons are related to the behavior discussed above regarding the non-availability of some of the heat absorbing reaction paths due to the absence of an intermediate species. While temperature changes are affected by gas dynamics, the water production is related to reaction rates at the specific temperature.

Figure 7 shows the profiles of the normalized mixture fractions, Z_H and Z_O, and their root mean square fluctuations across the mixing layer at 500 mm from the splitter plate and the pdf's of mixture fractions based on elements H and O. The Z_H profile shows monotonic behavior and the behavior of Z_O is not monotonic and this is consistent with the observation of Zheng.[9] The mean value of Z_O reaches the maximum value of 1.2 and the instantaneous values reach as high as 1.5 ($Z_O=1.5$ implies the element fraction of O, $z_O=0.23\times1.5=0.345$). For the mixture fraction formulation to be strictly valid, Z_H and Z_O must have identical behavior. Since Z_O shows non-monotonic behavior, it cannot be used as a convenient conserved scalar variable. Use of the mixture fraction in the literature seems not to indicate serious concern towards these features. The results of the present computations are used to assess the validity of the mixture fraction approach in spite of the non-normal diffusion of the species.

The probability density function of Z_H and Z_O have been calculated from the time series data of this variable at each

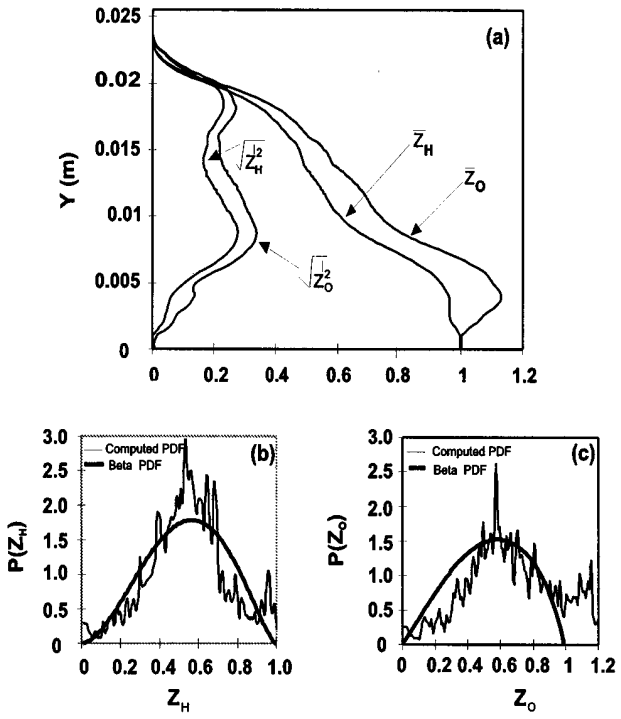

FIG. 7. The mean and rms fluctuations for mixture fractions of H and O and the pdf's computed from beta function and from numerical results.

location over one sweep duration and these are also shown in Fig. 7. The numerical pdf for H is reasonably well represented by the β function except near $Z_H=1$. Since Z_O goes above unity, the beta function cannot represent this pdf. For calculating the parameters of the density function this variable has been normalized with respect to the maximum value of Z_O and the resultant β-pdf is plotted in Fig. 7(c). Since the maximum varies from point to point this cannot be used for the purpose of modeling.

The plots of the mean z_H, z_O, and their rms fluctuations indicate a behavior in which the peak fluctuations are as large as 30%. Comparisons with Mach 2 experiments in co-flowing jets by Cheng *et al.*[2] indicate rms fluctuations in the mixture fraction of 0.1 or less. There are no other measurements available for comparison. Considering the hypervelocity environment of the flow and the dependence of dynamics of mixture fraction fluctuations on velocity fluctuations, the magnitude of the fluctuations may not be unreasonable.

Using the mixture fraction approach, the mean mass fractions of both Y_{H_2} and Y_{O_2} can be calculated from the computed time series of Z_H, either with fast chemistry approximations or with no reaction. The results are plotted in Fig. 8 along with the computed mean mass fractions of O_2 and H_2. For H_2, the three curves are very close to each other. This is because the major contribution to z_H comes from H_2 and the mass fraction of the element H in the products is small. The differences are more significant in Y_{O_2} profiles. The computed profiles lie between the fast chemistry and no-reaction profiles. The shapes of fast chemistry and the computed profiles are very similar. Hence, it might be concluded that mixture fraction approach can give reasonably

Downloaded 13 Feb 2007 to 203.200.43.195. Redistribution subject to AIP license or copyright, see http://pof.aip.org/pof/copyright.jsp

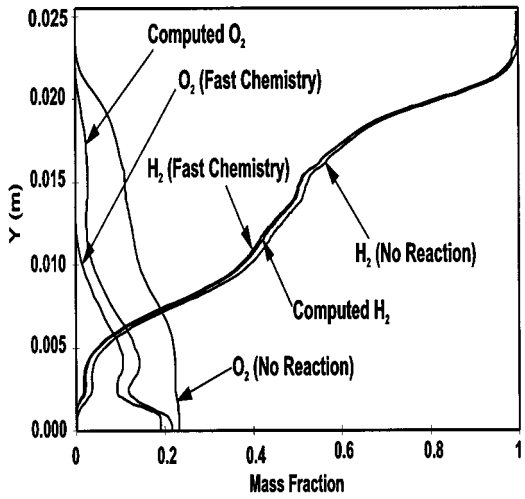

FIG. 8. A comparison of the mean mass fractions of H_2 and O_2 through the mixing layer for the no-reaction case and those obtained from the mixture fraction and fast chemistry approximations with FC results at $x=0.5$ m.

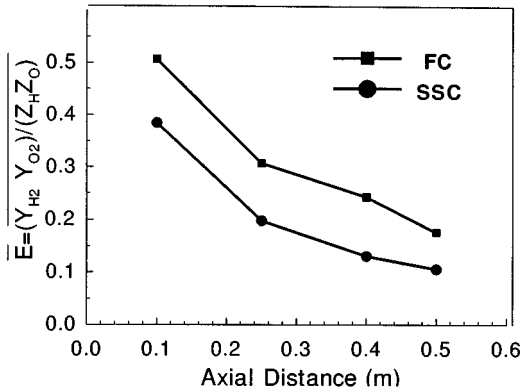

FIG. 10. Variation of $\overline{E}$ with an axial distance of $y=0.0127$ m.

accurate results for the reactants if finite chemistry effects are considered even though non-normal diffusion effects are significant.

Scatter plots of Y_{O_2} and Y_{H_2O} against the mixture fraction Z_H are shown in Fig. 9. Also plotted in the figure are the calculated mass fractions of these species for fast chemistry and no-reaction cases that the data are expected to lie within limits consistent with a mixture fraction formulation. All the computed points for O_2 lie between the limits, while many points for H_2O lie outside the limits. Experimental data by Cheng *et al.*[2] and Barlow *et al.*[30] show a similar behavior. This behavior is perhaps due to the diffusion effects. The contribution to the higher values of Z_O seem to be coming mainly from H_2O. Thus for product, the mixture fraction approach seems inadequate.

The time average of the quantity E at one lateral position is presented along the axis in Fig. 10 for both SSC and FC. It is clear that SSC is faster than FC. It is also clear that in both cases a reaction is yet to be completed. The conclusion that finite chemistry dominates the chemical behavior was asserted from short length simulations even for the case where high temperature air and fuel streams are the constituents in Ref. 21. This is consistent with the present study which indicates that ignition has just begun around 40 mm for what appear like more serious conditions and hydrogen being at as low a temperature as 103 K. It is no surprise to note the need for finite chemistry, either full or of the reduced kind, for describing the ignition zone or the processes following it in early stages.

The question as to whether the chemical processes in the mixing layer can be treated as belonging to fast chemistry, SSC, or FC limits and if the reduced chemistry model will be adequate is addressed presently.

(1) An examination of the contour plot of E for FC (shown in Fig. 5) has zones of unreacted fluid even in the far field.
(2) The reduction in the time average of E through the mixing layer for FC and a similar behavior for SSC allows one to conclude that even SSC can possibly simulate the overall behavior when a single measure is used to assess the quality of predictions. In the present case, a different choice of frequency factor, perhaps of activation energy, would able to predict the combustion process according to the quantity used in Fig. 10 or, if necessary, the average product flux at the exit.
(3) The use of reduced chemistry which can do well for ignition will do better in predicting a combustion process. The question is one of computational benefits vis-a-vis FC. As of now, there does not seem to be an adequate demonstration in the literature concerning this.

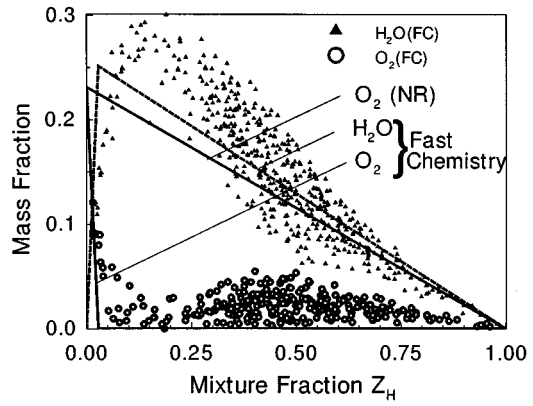

FIG. 9. Scatter plots of Z_H vs O_2 and H_2O mass fractions at $x=0.5$ m and $y=0.0127$ m.

V. CONCLUDING REMARKS

This paper has presented model-free computational results on a canonical problem in a hypervelocity nonpremixed reacting shear layer for which limited experimental results are available in the literature. The favourable comparisons of wall pressure are useful indicators for the goodness of computation, but the exploration of the chemistry–flow interaction is not entirely related to it. The examination of flow profiles shows the need to treat changes in kinetic

Downloaded 13 Feb 2007 to 203.200.43.195. Redistribution subject to AIP license or copyright, see http://pof.aip.org/pof/copyright.jsp

energy to predict the flow properties. The examination of flow pictures, the variation of the mixture fraction based on element H, the prediction of the mean mass fractions based on this mixture fraction, and a quantity to describe the progress of reaction ($Y_{H_2}Y_{O_2}/z_H z_0$) along the mixing layer all show that fast chemistry may be marginally inadequate in the present flow. The β probability density function is a good description of the fluctuations of mixture fraction. There are enough indications that the use of mixture fraction approach may be inadequate to compute high speed reacting turbulent flow.

ACKNOWLEDGMENT

The authors would like to express their sincere thanks to Dr. V. Adimurthy of VSSC, Thiruvananthapuram for the support provided for carrying out this work.

[1]M. C. Burrows and A. P. Kurkov, ''Analytical and experimental study of supersonic combustion in a vitiated air stream,'' NASA TM X-2828, 1993.
[2]T. Cheng, J. Wehrmeyer, R. Pitz, O. Jarret, Jr., and G. Northam, ''Finite rate chemistry effects in a Mach 2 reacting flow,'' AIAA-91-2320, 1991.
[3]J. Erdos, J. Tamagno, R. Bakos, and R. Trucco, ''Experiments on shear layer mixing at hypervelocity conditions,'' AIAA-92-0628, 1992.
[4]J. P. Drummond, ''Supersonic reacting internal flow fields,'' in *Numerical Approaches to Combustion Modeling*, edited by E. S. Oran and J. P. Boris, Progress in Astronautics and Aeronautics, 1991, Vol. 135, pp. 365–420.
[5]J. P. Drummond and M. H. Carpenter, ''Mixing and mixing enhancement in supersonic reacting flow fields,'' in *High Speed Flight Propulsion Systems*, edited by S. N. B. Murthy and E. T. Curran, Progress in Astronautics and Aeronautics, 1991, Vol. 137, pp. 383–455.
[6]B. Sekar and H. S. Mukunda, ''A computational study of direct simulation of high speed mixing layers without and with chemical heat release,'' *23rd Symposium (International) on Combustion*, 1991, The Combustion Institute, pp. 707–713.
[7]P. Vuillermoz, E. S. Oran, and K. Kailasnath, ''The effect of chemical reaction time on a supersonic reactive mixing layer,'' *24th Symposium (International) on Combustion*, 1992, The Combustion Institute, pp. 395–403.
[8]L. L. Zheng and K. N. C. Bray, ''Effects of dilatation dissipation on turbulent shear layer combustion in high speed flow,'' in Ref. 7, pp. 405–411.
[9]L. L. Zheng and K. N. C. Bray, ''The application of new combustion and turbulence models to H_2/air nonpremixed supersonic combustion,'' Combust. Flame **99**, 440 (1994).
[10]K. N. C. Bray, ''High speed turbulent combustion,'' in *Turbulent Reactive Flows*, edited by P. A. Libby and F. A. Williams (Academic Press, New York, 1994), pp. 609–638.
[11]J. S. Evans, C. J. Schexnayder, and H. L. Beach, ''Application of two-dimensional parabolic computer program to the prediction of turbulent reacting flows,'' NASA TP 1169, 1978.
[12]N. T. Clemens and M. G. Mungal, ''Two and three-dimensional effects in the supersonic mixing layer,'' AIAA-90-1978, 1990.
[13]S. A. Ragab and J. L. Wu, ''Linear instabilities in two-dimensional compressible mixing layers,'' Phys. Fluids A **1**, 957 (1989).
[14]N. D. Sandham and W. C. Reynolds, ''The compressible mixing layer: Linear theory and direct simulation,'' AIAA J. **28**, 618 (1990).
[15]C. K. W. Tam and F. Q. Hu, ''The instability and acoustic wave modes of supersonic mixing layers inside a recangular channel,'' J. Fluid Mech. **203**, 51 (1989).
[16]M. Zhuang, P. E. Dimotakis, and T. Kubota, ''The effect of walls on a spatially growing supersonic shear layer,'' Phys. Fluids A **2**, 599 (1990).
[17]D. Papamoschou and A. Roshko, ''The compressible turbulent shear layer: An experimental study,'' J. Fluid Mech. **197**, 453 (1988).
[18]P. J. Lu and K. C. Wu, ''Numerical investigation on the structure of a confined supersonic mixing layer,'' Phys. Fluids A **3**, 3063 (1991).
[19]T. Liou, W. Lien, and P. Hwang, ''Compressibility effects and mixing enhancement in turbulent free shear flows,'' AIAA J. **33**, 2332 (1995).
[20]Y. Ju and T. Niioka, ''Reaction kinetic mechanism of ignition for nonpremixed H_2/air in a supersonic mixing layer,'' Combust. Flame **99**, 240 (1994).
[21]H. S. Mukunda, ''Stretch effects in high speed mixing layers,'' Combust. Sci. Technol. **89**, 289 (1992).
[22]M. H. Carpenter, ''A generalised chemistry version of SPARK,'' NASA CR-4196, 1988.
[23]M. H. Carpenter and H. Kamath, ''Three dimensional extensions to the SPARK combustion code,'' NASP CP-5029, 1988.
[24]G. B. Northam and G. Y. Anderson, ''Supersonic combustion ramjet research at Langley,'' AIAA-86-0159, 1986.
[25]H. Yamashita, M. Shimada, and T. Takeno, ''A numerical study on flame stability at transition point of diffusion flames,'' *26th Symposium (International) on Combustion*, The Combustion Institute, 1996.
[26]P. E. Dimotakis and J. L. Hall, ''A simple finite chemical kinetics analysis of supersonic turbulent shear layer combustion,'' AIAA-87-1879, 1987.
[27]M. M. Koochesfahani, P. E. Dimotakis, and J. E. Broadwell, ''A 'Flip' experiment in a chemically reacting turbulent mixing layer,'' AIAA J. **23**, 1191 (1985).
[28]G. L. Brown and A. Roshko, ''On density effects and large structure in turbulent mixing layer,'' J. Fluid Mech. **64**, 775 (1974).
[29]P. E. Dimotakis, ''Turbulent free shear layer mixing,'' AIAA-89-0262, 1989.
[30]R. S. Barlow, R. W. Dibble, J. Y. Cheng, and R. P. Lucht, ''Effect of Damkohler number on superequilibrium OH concentration in turbulent non-premixed jet flame,'' Combust. Flame **82**, 235 (1990).

Downloaded 13 Feb 2007 to 203.200.43.195. Redistribution subject to AIP license or copyright, see http://pof.aip.org/pof/copyright.jsp